JCTA Journal of Computing Theories and Applications ISSN:3024-9104

Research Article

A Quantum Circuit Learning-based Investigation: A Case Study in Iris Benchmark Dataset Binary Classification

Muhamad Akrom *, Wise Herowati, and De Rosal Ignatius Moses Setiadi

Research Center for Quantum Computing and Materials Informatics, Faculty of Computer Science, Dian Nuswantoro University, Semarang 50131, Indonesia; e-mail: m.akrom@dsn.dinus.ac.id; wise@dsn.dinus.ac.id; moses@dsn.dinus.ac.id

* Corresponding Author: Muhamad Akrom

Abstract: This study presents a Quantum Machine Learning (QML) architecture for perfectly classifying the Iris flower dataset. The research addresses improving classification accuracy using quantum models in machine-learning tasks. The objective is to demonstrate the effectiveness of QML approaches, specifically the Variational Quantum Circuit (VQC), Quantum Neural Network (QNN), and Quantum Support Vector Machine (QSVM), in achieving high performance on the Iris dataset. The proposed methods result in perfect classification, with all models attaining accuracy, precision, recall, and an F1-score of 1.00. The main finding is that the QML architecture successfully achieves flawless classification, contributing significantly to the field. These results underscore the potential of QML in solving complex classification problems and highlight its promise for future applications across various domains. The study concludes that QML techniques can offer transformative solutions in machine learning tasks, particularly those leveraging VQC, QNN, and QSVM.

Keywords: Iris Dataset; Quantum Classification; Quantum Machine Learning; Quantum Neural Network; Quantum Support Vector Machine; Variational Quantum Circuit.

1. Introduction

Quantum computation has gained popularity due to its numerous applications, leveraging non-classical features of quantum states [1]–[6]. Some tasks lack classical counterparts, while others show significant quantum advantages[7]–[9]. Entanglement and superposition are vital principles that have redefined how information is represented in quantum computation. Quantum computers differ from ordinary computers in using qubits instead of bits. Qubits, the fundamental units of information, are inherently complex, allowing quantum computers to handle tasks that regular systems cannot. Qubits have computational capabilities that outperform conventional computing due to superposition and entanglement, indicating a considerable departure from the field[10]–[13].

Superposition allows qubits to exist in states representing both 0 and 1 simultaneously. This feature enables quantum computers to perform complex calculations while exploring multiple possibilities simultaneously [14]–[16]. Equation $|\psi\rangle = \alpha|0\rangle + \beta|1\rangle$ illustrates a qubit's quantum state, highlighting its ability to exist in several states simultaneously. This distinguishes quantum computing from classical paradigms and further proves quantum systems' enhanced computational capabilities. $|\psi\rangle$ represents the quantum state of a qubit in a two-dimensional complex Hilbert space, with basis vectors $|0\rangle$ and $|1\rangle$. The coefficients α and β determine the qubit's superposition in the states $|0\rangle$ and $|1\rangle$. Entanglement is a critical notion that characterizes the dependency between the states of numerous qubits. It allows quantum computers to excel at processing massive datasets and addressing specific computational issues[17], [18].

Machine learning (ML) is effective for data classification, regression, and clustering [19]–[25]. However, applying quantum principles to ML is challenging. Quantum circuit learning (QCL), also known as quantum ML (QML), is a growing field combining quantum computing with ML [26], [27]. QML algorithms can be built as quantum circuits with various quantum

Received: November, 25th 2024
Revised: December, 25th 2024
Accepted: January, 1st 2024
Published: January, 5th 2024

gate operations[28]–[30]. In addition to purely quantum approaches, hybrid quantum-classical methods have been proposed to harness the complementary strengths of quantum and classical computation. These hybrid methods often utilize quantum circuits for tasks like feature encoding and rely on classical optimization algorithms to adjust model parameters[31]–[34]. QML can advance quantum computing in the noisy intermediate-scale quantum (NISQ) era, offering significant advantages over classical methods, especially for near-term quantum devices [29], [35] the development of pure quantum methodologies capable of processing classical data entirely within a quantum framework remains a more complex and less explored challenge.

This study investigates QML performances for classifier tasks using a supervised learning technique on the Iris dataset as an experiment. We propose three QML architectures in this evaluation, namely adaptive quantum neural network (AQNN), variational quantum circuit (VQC), and quantum support vector machine (QSVM). Unlike hybrid approaches, this research focuses on processing classical data entirely within a quantum system, highlighting pure quantum methods' unique challenges and opportunities. The contributions of this study are as follows:

1. Proposal of QML architectures, including AQNN, VQC, and QSVM, tailored for binary classification tasks.
2. Evaluation of the performance of pure quantum approaches in processing classical data for classification.
3. Demonstrating the challenges and potential of implementing purely quantum solutions within a supervised learning context.

The rest of this paper is organized into Section 2, which discusses related work, focusing on studies utilizing quantum and hybrid quantum-classical methods. Section 3 elaborates on the proposed methodologies, including dataset preparation, model design, and evaluation. Section 4 presents results and discussion, and Section 5 concludes the study with future directions.

2. Related Works

Quantum machine learning (QML) represents a growing intersection between quantum computing and classical machine learning, enabling solutions to complex problems by leveraging quantum phenomena such as superposition and entanglement, a foundational study by Schuld et al. [27] and Havlíček et al. [28] introduced quantum-enhanced feature spaces, demonstrating the potential of quantum kernels in supervised learning. These works established a framework for integrating quantum properties to enhance the expressiveness of machine learning models.

The development of PQC, as discussed by Mitarai et al.[36], further advanced QML by optimizing quantum gate parameters for specific learning tasks. PQC has shown adaptability across various machine learning paradigms, including classification and regression, and remains a cornerstone for QML architectures.

Hybrid quantum-classical methods have also gained attention. For instance, Tomal et al. [33] proposed a Quantum Convolutional Neural Network (QCNN) that combines quantum feature extraction with classical layers for classification, achieving significant improvements in model accuracy. Similarly, Safriandono et al. [34] explored hybrid frameworks for integrating temporal and quantum features, highlighting the synergy between quantum encoding and classical optimization.

While hybrid approaches effectively harness the strengths of quantum and classical computation, fully quantum methods are less explored. Schuld and Killoran [29] highlighted the potential of processing data entirely within quantum domains, emphasizing the role of quantum feature spaces and optimization techniques. This aligns with the growing need to investigate pure quantum methodologies that bypass classical dependencies, offering direct advantages for quantum-native applications.

This study builds upon these advancements by focusing on fully quantum approaches, using VQC, QNN, and QSVM to process classical data in a purely quantum framework. Unlike prior works that relied on hybrid systems, our research addresses the underexplored challenges of encoding classical data into quantum states and optimizing quantum-specific architectures for machine learning tasks.

3. Proposed Method

In this work, we implement quantum operations developed using the Qiskit module on quantum hardware in the IBM Quantum platform.

3.1. Dataset and preprocessing

The Iris dataset is a well-known benchmark in machine learning, frequently utilized for data classification tasks. It comprises 150 samples of iris flowers, each characterized by four features: sepal length, sepal width, petal length, and petal width. These samples are categorized into three distinct classes, each representing a different species of iris: Iris setosa, Iris versicolor, and Iris virginica, with 50 samples per class. To perform binary classification using the Iris dataset, we initiated a preprocessing stage in which we selected two of the three courses. Specifically, we chose the classes Iris setosa and Iris versicolor, while excluding the third class, Iris virginica.

Another preprocessing stage includes normalizing the data using the Min-MaxScaler to address model sensitivity issues and reduce prediction errors [37]–[39]. Next, the dataset is divided into training and test sets to enable model training and evaluation[40]. This step involves splitting the normalized data into a ratio of 70% for training and 30% for testing, ensuring that the model is trained on a subset of the data and validated on a separate subset to assess its performance[41]–[43].

2.2. QML Modeling

Recalibrating within the context of QML is necessary for integrating quantum-based programming to make it executable on a quantum computer. The QML method is a quantum version of the classical ML based on the ideas of quantum mechanics. Investigating QML's potential for classification prediction is the main objective of the proposed endeavor. Figure 1 shows the architecture of the proposed QML.

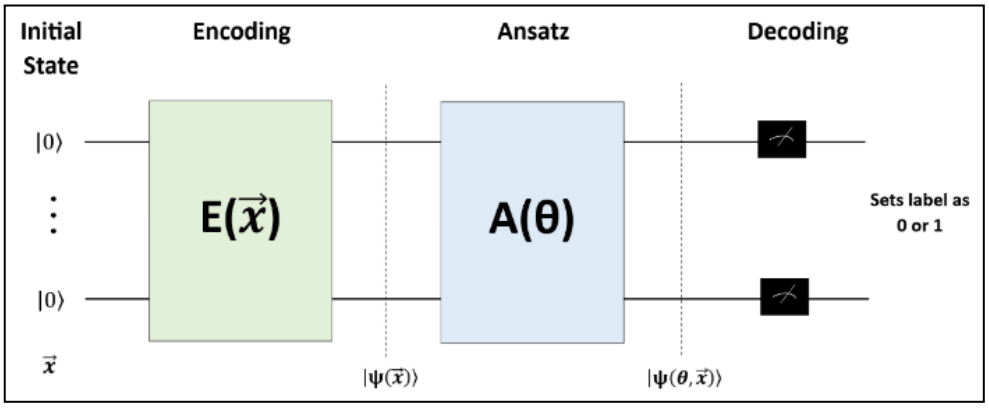

Figure 1. The architecture of the proposed QML

According to Figure 1, the first step of the QML approach is assigning qubits to each feature in the data. Next, each feature is mapped, which is also referred to as encoding. This is a basic phase in which quantum feature mapping is used to build a quantum state in the quantum Hilbert space[44], [45]. This technique brings qubits into many states of superposition and entanglement. The quantum feature mapping, $\mathrm{E}(\vec{x})$, as described in Equation (1), encodes the classical input vector $\vec{x}$ into the quantum state vector $|\psi(\vec{x})\rangle$ for each observation by applying it to the ground state $|0\rangle$ for each qubit. In essence, every classical characteristic is associated with a single qubit.

$$\mathrm{E}(\vec{x})|0\rangle = |\psi(\vec{x})\rangle \tag{1}$$

After classical characteristics are first encoded into quantum states, an ansatz represented by $\mathrm{A}(\theta)$. QML uses equation (2) to perform classification by evaluating the degree of similarity between data vectors in the quantum feature space[46], [47].

$$\mathrm{A}(\theta)|\psi(\vec{x})\rangle = |\psi(\theta,\vec{x})\rangle \tag{2}$$

Binary value encodings translate quantum state data into traditional values of 0 and 1 once the classifier has been fitted[48], [49]. Parameterized (θ) are also adjusted to reduce loss function.

2.3. Model Assessment

ROC curves, recall, F1-score, accuracy, and precision are important for assessing classifier models. The ratio of accurate forecasts to total predictions is known as accuracy. Recall evaluates the percentage of genuine positive predictions among all real positives, whereas precision measures the percentage of true positive forecasts across all positive predictions. The F1-score, the harmonic mean of accuracy and recall, balances these two measures. ROC curves illustrate performance across thresholds by plotting the true positive rate versus the false positive rate[44], [50], [51].

$$Accuracy = \frac{(TP + TN)}{(TP + TN + FP + FN)} \times 100 \tag{3}$$

$$Precision = \frac{TP}{(TP + FP)} \times 100 \tag{4}$$

$$Recall\ (Sensitivity) = \frac{TP}{(TP + FN)} \times 100 \tag{5}$$

$$F1 - Score = \frac{2 \times Precision \times Recall}{(Precision + Recall)} \tag{6}$$

In this case, true positives are indicated by TP, true negatives by TN, false positives by FP, and false negatives by FN. These metrics thoroughly assess the model's functionality and predicted accuracy inside a classification framework, giving important information about how well the model can accurately categorize instances into various groups.

2.4. Parameter Optimization

In QNN, feature mapping parameters and ansatz are based on adaptive circuit development involving custom circuit structure variations. For VQC and QSVM, feature mapping parameters are based on variational circuits, such as PauliFeatureMap and ZFeatureMap. These feature mapping parameters enable the search for the best data encoding, effectively converting classical data into more informative quantum representations. In VQC classification tasks, quantum circuit-based variational parameters such as RealAmplitudes, EfficientSU2, and TwoLocal are used to find the optimal ansatz structure for processing input data. For QSVM, the basis for ansatz optimization is the selection of quantum kernels, such as FidelityQuantumKernel and FidelityStatevectorKernel. Optimizing encoding parameters and ansatz helps to solve effective data classification tasks by evaluating the similarity between data pairs in the quantum feature space, thereby improving the model's ability to learn and classify data.

Gradient optimization is also added to adjust the parameters in the model to minimize the loss function using several optimization algorithms such as adaptive moment estimation (ADAM), constrained optimization by linear approximations (COBYLA), and analytic quantum gradient descent (AQGD). By computing and updating the gradient of the loss function, quantum models can iteratively improve their performance in classification tasks, ensuring more informative quantum feature mappings and optimal ansatz for data processing.

4. Results and Discussion

4.1. Variational Quantum Circuit (VQC)

We begin a series of experiments by assessing how well various VQC models perform in categorizing the Iris dataset. The findings indicate that the model's performance varies based on the circuit parameterization and design employed.

The results are presented in Table 1. Based on the data in Table 1, the VQC_6 model using ZFeatureMap as the encoding and EfficientSU2 as the ansatz has shown a maximum accuracy of 87.5%. This combination captures the variations and patterns of the Iris dataset rather well. The most efficient ansatz is EfficientSU2, which produces the best outcomes with ZFeatureMap and PauliFeatureMap encodings. With any encoding, RealAmplitudes and TwoLocal do not perform well enough, suggesting that they must be modified further or used in other situations.

Table 1. Performance of the VQC models using ADAM as an optimizer.

Model	Encoding	Ansatz	Accuracy
VQC1	PauliFeatureMap	TwoLocal	0.550
VQC2	PauliFeatureMap	RealAmplitudes	0.538
VQC3	PauliFeatureMap	EfficientSU2	0.800
VQC4	ZFeatureMap	TwoLocal	0.562
VQC5	ZFeatureMap	RealAmplitudes	0.688
VQC6	ZFeatureMap	EfficientSU2	0.875

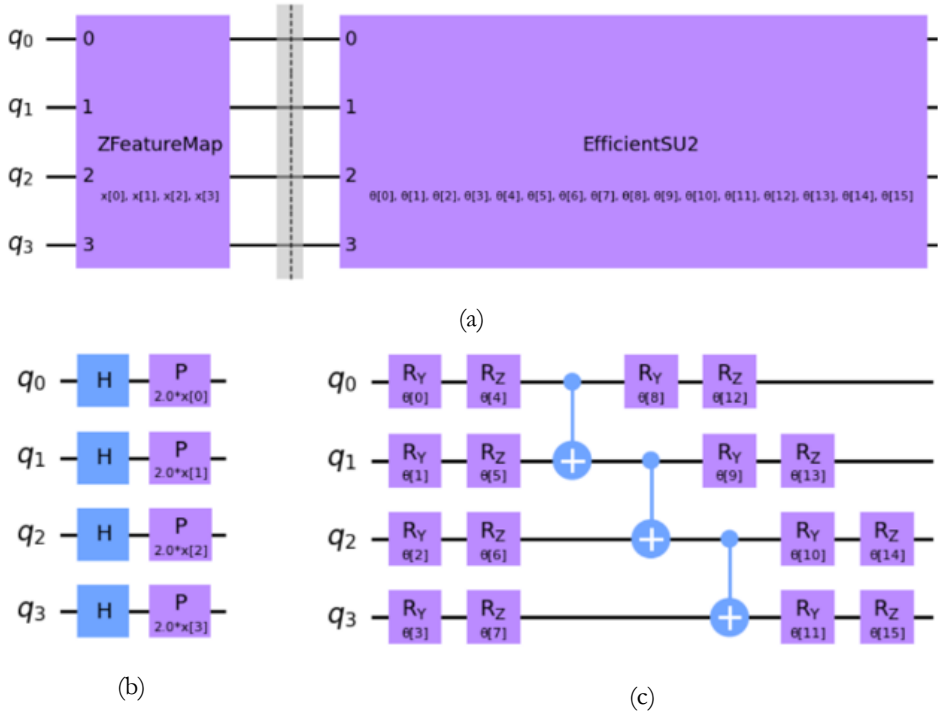

Figure 2. (**a**) Structure of VQC_6 model; (**b**) ZfeatureMap as encoding; (**c**) EfficientSU2 as ansatz.

Figure 2a illustrates the architecture of the VQC_6 model, which integrates a ZFea-tureMap quantum circuit as the encoding mechanism and an EfficientSU2 quantum circuit as the ansatz. The amalgamation of quantum gates comprising ZFeatureMap and EfficientSU2 facilitates the effective extraction of information from the dataset. ZFeatureMap is assembled from Hadamard (H) and phase (P) gates to convert input features into quantum representations. The H gate induces a superposition state, enabling simultaneous information exploration across multiple feature dimensions. Meanwhile, the P gate introduces the phase to the quantum state, enhancing the projection of feature information into a larger Hilbert space. EfficientSU2 comprises parametric gates, single-qubit gates Ry and Rz, and a two-qubit gate CX. The Ry and Rz gates facilitate rotations about the y-axis and z-axis, respectively, enabling rotational transformations on quantum states within the Hilbert space. The CX gate establishes correlations between two qubits in the circuit, facilitating intricate quantum operations such as entanglement. The synergy of these gates within an ansatz enables the creation of complex and adaptable circuit structures. Consequently, the fusion of ZFeatureMap for encoding and Ef-ficientSU2 gates for ansatz within the VQC_6 model adeptly captures the

variations and patterns present in the Iris dataset. This combination leverages the inherent capabilities of quantum gates to efficiently represent and process data, thereby enhancing the model's performance in classification tasks.

Various optimizers were used to optimize the best VQC model (VQC_6), including ADAM, COBYLA, and AQGD. AQGD achieved the highest accuracy at 100%, attributed to its precise tracking of the loss function landscape. In contrast, ADAM and COBYLA achieved 87.5% and 97.5% accuracy, respectively. ADAM's lower performance is due to its less precise adaptive capabilities, while COBYLA's linear optimization method is simpler and less effective than AQGD's approach. This experiment underscores the crucial role of optimizer selection in VQC model performance, with AQGD proving to be the most effective, followed by COBYLA. Despite its popularity in classical machine learning, ADAM performed poorly in this quantum context, highlighting the importance of using optimizers tailored for quantum models.

Table 2. Expressibilty value of ansatzes

Circuit	Expressibility
TwoLocal	0.10
RealAmplitudes	0.07
EfficientSU2	0.05

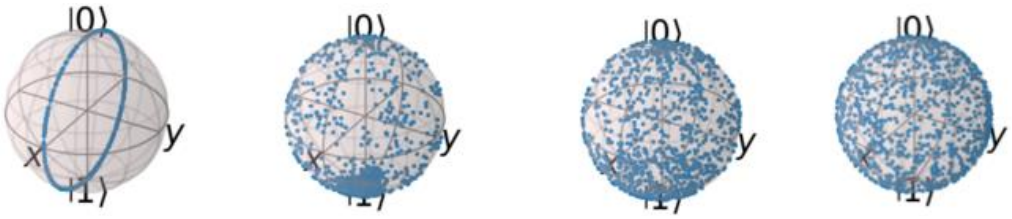

(a) (b) (c) (d)

Figure 3. Bloch's representation of expressibility for variational circuits (**a**) TwoLocal; (**b**) RealAmplitudes; (**c**) EfficientSU2; (**d**) Haar.

The Haar measure defines a uniform distribution over unitary operators, essential for assessing quantum circuit expressibility. A Haar random state uniformly samples the Hilbert space, representing maximal expressibility. Comparing quantum circuits to the Haar measure gauges their effectiveness in exploring the quantum state space. Based on Table 2, EfficientSU2 is the most capable of generating a broad distribution akin to Haar random states, making it optimal for variational quantum algorithms. RealAmplitudes offers a balanced approach, while TwoLocal is less effective in state space exploration. According to Figure 3, EfficientSU2 circuits best approximate the Haar measure, providing a uniform state distribution on the Bloch sphere, which makes them ideal for variational quantum algorithms.

4.2. Adaptive Quantum Neural Network (AQNN)

Following the experimentation with the VQC model, the study progressed by constructing three AQNN models.

Table 3. Performance of the AQNN model using ADAM as an optimizer

Model	Accuracy
AQNN_1	0.525
AQNN_2	0.693
AQNN_3	0.858

The results presented in Table 3 reveal a progressive enhancement in performance from AQNN_1 to AQNN_3. Notably, AQNN_3 attains the highest accuracy, achieving a commendable 85.8%. This notable performance escalation underscores the success of quantum model adaptation in AQNN_3, allowing for a more proficient capture of data patterns and

features compared to its counterparts. The observed improvement in performance can be primarily attributed to the AQNN_3 model's adeptness at adaptively learning from input data. By leveraging quantum mechanisms for adaptation, AQNN_3 exhibits an enhanced capability to discern intricate patterns within the dataset, leading to superior classification accuracy. Thus, this experimentation underscores the potential of quantum model adaptation in augmenting performance for data processing and classification tasks. The results highlight the promising avenues for leveraging quantum computing techniques to advance the efficiency and efficacy of machine learning models, paving the way for transformative advancements in data analytics and classification methodologies.

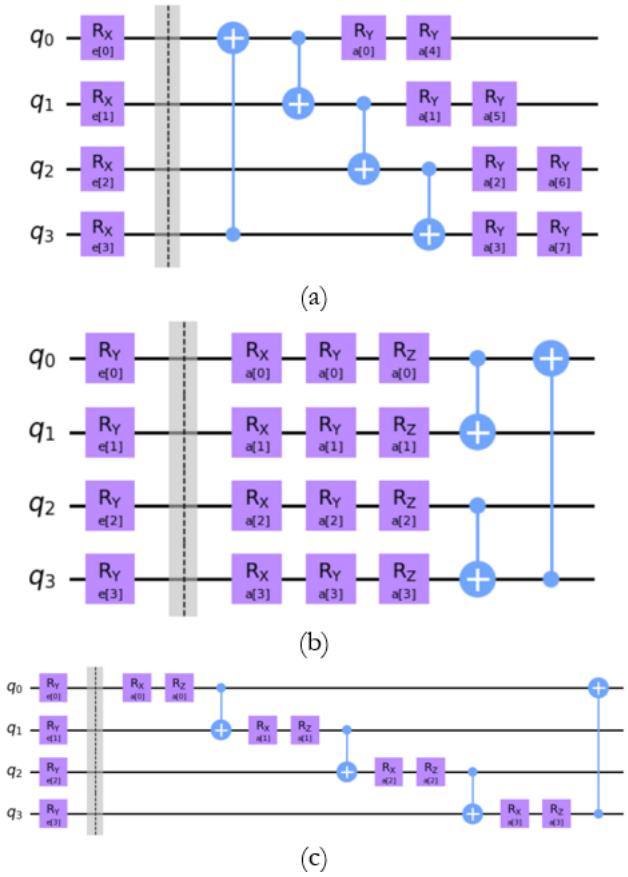

Figure 4. Construction of (**a**) AQNN_1; (**b**) AQNN_2; and (**c**) AQNN_3 models.

The performance discrepancies observed among the AQNN models can be elucidated through their distinct encoding and ansatz configurations in Figure 4. The AQNN_1 model employs Rx gates for encoding and a circuit combining Ry and CX gates for the ansatz. Despite its simplicity with a singular encoding gate type, this model exhibits relatively low accuracy. This suggests that utilizing a more intricate circuit structure or incorporating diverse encoding gates may be necessary to effectively capture the intricate patterns in the data. In contrast, the AQNN_2 model utilizes Ry gates for encoding and a more elaborate ansatz circuit comprising Rx, Ry, Rz, and CX gates. Leveraging a broader spectrum of encoding gates and a complex ansatz circuit, this model demonstrates a notable enhancement in accuracy compared to AQNN_1. Similarly, the AQNN_3 model adopts Rx gates for encoding, akin to AQNN_1, but features a sophisticated ansatz circuit integrating Rx, Rz, and CX gates. Despite sharing the same encoding type as AQNN_1, including a more intricate ansatz structure enables AQNN_3 to achieve substantially higher accuracy. This underscores the pivotal role of a well-designed circuit structure in augmenting the performance of quantum models. Hence, the elevated accuracy achieved by the AQNN_2 and AQNN_3 models, compared to AQNN_1, underscores the significance of judiciously selecting both gate encoding and ansatz circuit structures in optimizing the performance of quantum models. This

emphasizes the necessity of tailoring quantum circuits to the specific characteristics of the dataset to capture and leverage its underlying patterns effectively.

After identifying the AQNN_3 model as the most promising, optimization efforts were undertaken utilizing various optimizers, namely ADAM, AQGD, and COBYLA. The findings revealed that COBYLA achieved the highest accuracy of 100.0%, followed closely by AQGD with an accuracy of 96.2%, while ADAM trailed behind with an accuracy of 85.8%. This underscores the pivotal role of optimizer selection in enhancing the performance of the AQNN_3 model. The results highlight COBYLA as the optimal optimizer for the AQNN_3 model within this framework, as it attains the highest accuracy. Nevertheless, AQGD also demonstrates commendable performance, boasting near-perfect accuracy.

In contrast, ADAM exhibits inferior performance compared to other optimizers. This underscores the criticality of aligning the choice of optimizer with the inherent characteristics of the quantum model and the specific dataset under consideration. By selecting an optimizer that synergizes effectively with the model's architecture and the dataset's intricacies, optimal performance can be attained, thereby maximizing the model's efficacy in classification tasks.

4.3. Quantum Support Vector Machine (QSVM)

Table 4 summarizes the results of evaluating the QSVM model with PauliFeatureMap and ZFeatureMap encodings, employing the FidelityQuantumKernel ansatz.

Table 4. Performance of the QSVM models using ADAM as an optimizer and FidelityQuantumKernel as ansatz

Model	Accuracy
AQSVM_1	0.988
AQSVM_2	0.990

Notably, QSVM_2 exhibits superior accuracy compared to QSVM_1. This delineates the efficacy of utilizing ZFeatureMap encoding in conjunction with the FidelityQuantumKernel ansatz, yielding commendable performance in data classification. Conversely, the fusion of PauliFeatureMap with the same ansatz yields competitive accuracy. This observation underscores the pivotal role of encoding and ansatz selection in QSVM, significantly influencing model performance. These findings offer valuable insights into refining quantum models tailored for classification tasks. By discerningly choosing encoding and ansatz configurations, researchers can harness the full potential of quantum computing in optimizing model accuracy and efficacy in classification endeavors.

After evaluating the QSVM_2 model with various optimizers, namely ADAM, COBYLA, and AQGD, the resulting accuracies were 99.0%, 100.0%, and 100.0%, respectively. This signifies a notable improvement, although it falls short of achieving perfect accuracy. The COBYLA and AQGD optimizers emerged as the best for the QSVM_2 model, each attaining ideal accuracy. This underscores the significant impact optimizers designed explicitly for quantum contexts can have on model performance. While ADAM demonstrated competitive performance, it did not match the perfection of COBYLA and AQGD. These results highlight the critical importance of selecting appropriate optimizers to achieve optimal performance in quantum models. The effectiveness of COBYLA and AQGD in this experiment confirms their suitability for QSVM model optimization, providing valuable insights for future developments in QML.

4.4. Comparison of Model Performances

Table 5 exhibits the performance metrics of VQC, QNN, and QSVM, wherein each model's accuracy, precision, recall, and F1-score are meticulously documented, all demonstrating an exemplary performance denoted by a perfect value of 1.00 across all metrics for each model. This impeccable performance observed across all models and metrics warrants considerable attention. It implies various conceivable scenarios, notably the potential separability of the utilized dataset for training and testing through the chosen quantum models. This signifies the presence of well-defined decision boundaries between distinct classes within the dataset, thereby facilitating the models' attainment of flawless classification performance. Furthermore, the employed models, namely VQC, QNN, and QSVM, exhibit adequate

complexity to accurately capture the underlying patterns inherent in the data. Leveraging a quan-tum-based framework, these models inherently possess an augmented capacity to comprehend and depict intricate relationships embedded within the dataset.

Table 5. Comparison of QML model performances.

Model	Accuracy	Precision	Recall	F1-score
VQC	1.00	1.00	1.00	1.00
QNN	1.00	1.00	1.00	1.00
QSVM	1.00	1.00	1.00	1.00

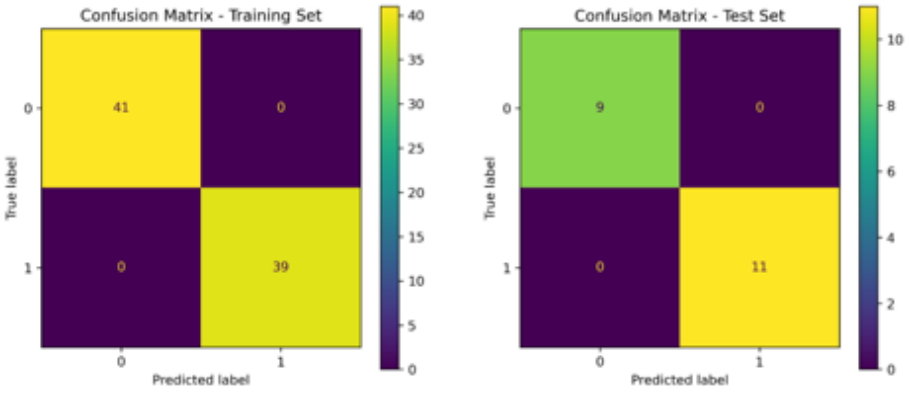

(a)

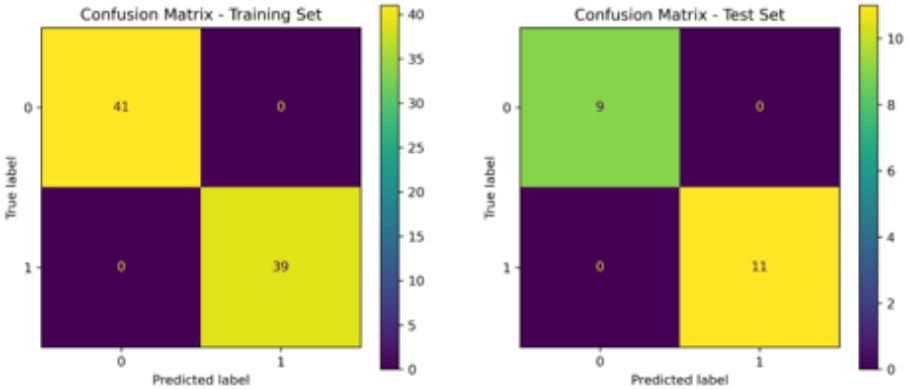

(b)

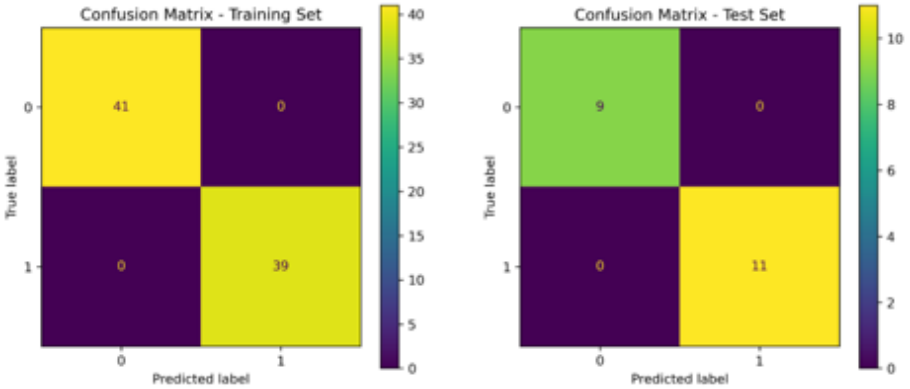

(c)

Figure 5. Confusion matrix of models (**a**) VQC; (**b**) QNN; (**c**) QSVM.

The confusion matrix is essential for comprehending a classification model's performance. It sheds light on the model's many TP, TN, FP, and FN predictions. The performance of each model is thoroughly understood by looking at the confusion matrix (Figure 5). Each row in the matrix represents an actual event, and each column represents a predicted occurrence. Accurately categorized instances lay off the diagonal, whereas predictably classified instances lie on it. Analyzing the confusion matrix for each model can provide deeper insights into their performance, especially in scenarios where all other metrics are perfect. The confusion matrix displays the counts of true positives (TP), true negatives (TN), false positives (FP), and false negatives (FN) for each class. From Figure 5, the confusion matrices show only diagonal elements, indicating perfect classification for three models.

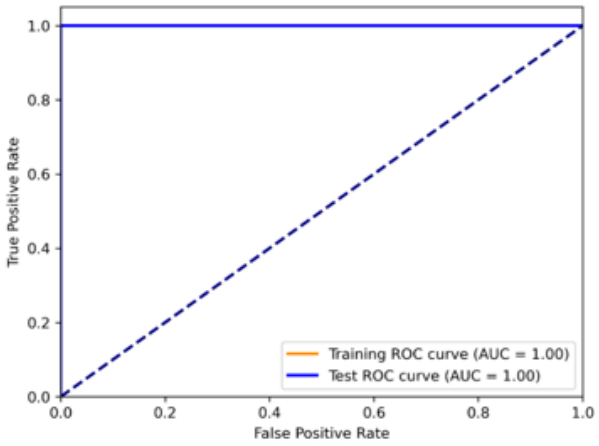

(a)

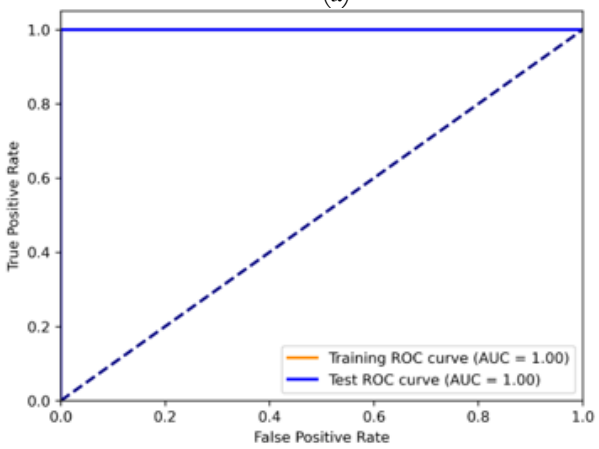

(b)

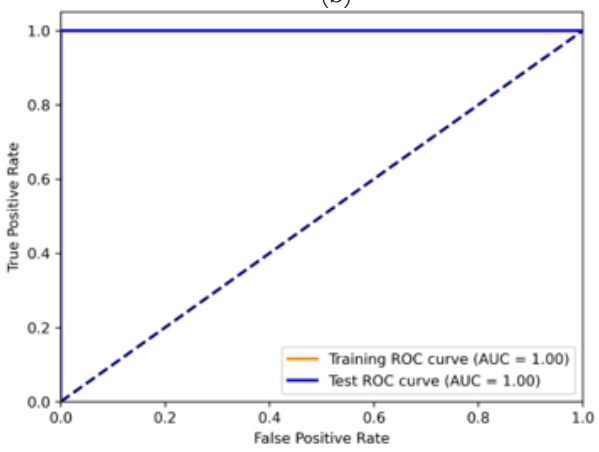

(c)

Figure 6. ROC-AUC of models (**a**) VQC; (**b**) QNN; (**c**) QSVM.

The performance of a classifier is represented graphically by the receiver operating characteristic (ROC) curve. At different threshold values, it shows the TP rate (recall) versus the FP rate (1 - specificity). A single scalar number, 1.00 denoting a perfect classifier and 0.50 denoting a random classifier, is the area under the curve (AUC), which summarizes the classifier's performance. ROC curve and AUC are additional evaluation metrics that provide insights into the models' performance, particularly in binary classification tasks. From Figure 6, it's reasonable if the ROC curves will display perfect performance for all models. In a scenario where AUC is perfect (1.00), the ROC curve will typically show a point at (0; 1) on the graph, indicating perfect classification with no false positives and no false negatives. This point represents the ideal operating point where the true positive rate (sensitivity) is 1, and the false positive rate is 0. It's important to note that the perfect AUC (1.00) suggests that the models have achieved the best possible discrimination between positive and negative classes, indicating excellent separability in the dataset.

5. Conclusions

This study investigated the effectiveness of QML models, including VQC, QNN, and QSVM, in achieving accurate binary classification on the Iris dataset. The results demonstrated that all three models achieved perfect classification performance, with accuracy, precision, recall, F1-score, and AUC reaching 1.00. These findings confirm that the proposed QML approaches successfully address the challenges of processing classical data entirely within a quantum framework. The models effectively captured and represented the underlying patterns of the dataset, validating their capability to handle classification tasks in a fully quantum manner. Additionally, the performance consistency across models highlights the robustness and reliability of the methodologies employed.

Furthermore, the study underscores the practicality of QML models in leveraging quantum principles such as superposition and entanglement to enhance classification accuracy. Evaluating different ansatz structures, encoding mechanisms, and optimization strategies also provided valuable insights into the factors contributing to the models' success. The results indicate that the research objectives have been successfully met, demonstrating the viability and potential of fully quantum approaches in machine learning applications. These findings open opportunities for further exploration of QML techniques across diverse datasets and problem domains and for developing more advanced quantum hardware to support larger-scale tasks.

Author Contributions: MA, WH, DRIMS: designed quantum circuit, experiment, performed analysis, MA: reviewed, supervised. All authors contributed to the final manuscript.

Funding: This research received no external funding.

Acknowledgments: All calculations were performed using the Computation Facility at the Research Center for Quantum Computing and Materials Informatics, Universitas Dian Nuswantoro, and IBM Quantum Experience.

Conflicts of Interest: The authors declare that they have no known competing financial or non-financial interests or personal relationships that could have appeared to influence the work reported in this paper.

References

[1] R. D. M. Simoes, P. Huber, N. Meier, N. Smailov, R. M. Fuchslin, and K. Stockinger, "Experimental Evaluation of Quantum Machine Learning Algorithms," *IEEE Access*, vol. 11, pp. 6197–6208, 2023, doi: 10.1109/ACCESS.2023.3236409.

[2] N. Nguyen and K.-C. Chen, "Quantum Embedding Search for Quantum Machine Learning," *IEEE Access*, vol. 10, pp. 41444–41456, 2022, doi: 10.1109/ACCESS.2022.3167398.

[3] A. Zeguendry, Z. Jarir, and M. Quafafou, "Quantum Machine Learning: A Review and Case Studies," *Entropy*, vol. 25, no. 2, p. 287, Feb. 2023, doi: 10.3390/e25020287.

[4] E. Grant *et al.*, "Hierarchical quantum classifiers," *npj Quantum Inf.*, vol. 4, no. 1, p. 65, Dec. 2018, doi: 10.1038/s41534-018-0116-9.

[5] A. Chalumuri, R. Kune, and B. S. Manoj, "A hybrid classical-quantum approach for multi-class classification," *Quantum Inf. Process.*, vol. 20, no. 3, p. 119, Mar. 2021, doi: 10.1007/s11128-021-03029-9.
[6] S. Adhikary, S. Dangwal, and D. Bhowmik, "Supervised learning with a quantum classifier using multi-level systems," *Quantum Inf. Process.*, vol. 19, no. 3, p. 89, Mar. 2020, doi: 10.1007/s11128-020-2587-9.
[7] L. K. Grover, "A fast quantum mechanical algorithm for database search," in *Proceedings of the twenty-eighth annual ACM symposium on Theory of computing - STOC '96*, 1996, pp. 212–219. doi: 10.1145/237814.237866.
[8] A. K. Ekert, "Quantum cryptography based on Bell's theorem," *Phys. Rev. Lett.*, vol. 67, no. 6, pp. 661–663, Aug. 1991, doi: 10.1103/PhysRevLett.67.661.
[9] M. Akrom, S. Rustad, and H. K. Dipojono, "Variational quantum circuit-based quantum machine learning approach for predicting corrosion inhibition efficiency of pyridine-quinoline compounds," *Mater. Today Quantum*, vol. 2, p. 100007, Jun. 2024, doi: 10.1016/j.mtquan.2024.100007.
[10] H. Ma, J. Liu, H. Shang, Y. Fan, Z. Li, and J. Yang, "Multiscale quantum algorithms for quantum chemistry," *Chem. Sci.*, vol. 14, no. 12, pp. 3190–3205, 2023, doi: 10.1039/D2SC06875C.
[11] B. A. Alhayani, O. A. AlKawak, H. B. Mahajan, H. Ilhan, and R. M. Qasem, "Design of Quantum Communication Protocols in Quantum Cryptography," *Wirel. Pers. Commun.*, Jul. 2023, doi: 10.1007/s11277-023-10587-x.
[12] Z. Deng, X. Wang, and B. Dong, "Quantum computing for future real-time building HVAC controls," *Appl. Energy*, vol. 334, p. 120621, Mar. 2023, doi: 10.1016/j.apenergy.2022.120621.
[13] A. Pyrkov *et al.*, "Quantum computing for near-term applications in generative chemistry and drug discovery," *Drug Discov. Today*, vol. 28, no. 8, p. 103675, Aug. 2023, doi: 10.1016/j.drudis.2023.103675.
[14] P. Brown and H. Zhuang, "Quantum machine-learning phase prediction of high-entropy alloys," *Mater. Today*, vol. 63, pp. 18–31, Mar. 2023, doi: 10.1016/j.mattod.2023.02.014.
[15] J. Biamonte, P. Wittek, N. Pancotti, P. Rebentrost, N. Wiebe, and S. Lloyd, "Quantum machine learning," *Nature*, vol. 549, no. 7671, pp. 195–202, Sep. 2017, doi: 10.1038/nature23474.
[16] M. Akrom, S. Rustad, and H. K. Dipojono, "Development of quantum machine learning to evaluate the corrosion inhibition capability of pyrimidine compounds," *Mater. Today Commun.*, vol. 39, p. 108758, Jun. 2024, doi: 10.1016/j.mtcomm.2024.108758.
[17] H. Gupta, H. Varshney, T. K. Sharma, N. Pachauri, and O. P. Verma, "Comparative performance analysis of quantum machine learning with deep learning for diabetes prediction," *Complex Intell. Syst.*, vol. 8, no. 4, pp. 3073–3087, Aug. 2022, doi: 10.1007/s40747-021-00398-7.
[18] T. Suzuki and M. Katouda, "Predicting toxicity by quantum machine learning," *J. Phys. Commun.*, vol. 4, no. 12, p. 125012, Dec. 2020, doi: 10.1088/2399-6528/abd3d8.
[19] Y. LeCun, Y. Bengio, and G. Hinton, "Deep learning," *Nature*, vol. 521, no. 7553, pp. 436–444, May 2015, doi: 10.1038/nature14539.
[20] M. Akrom, S. Rustad, and H. Kresno Dipojono, "Prediction of Anti-Corrosion performance of new triazole derivatives via Machine learning," *Comput. Theor. Chem.*, vol. 1236, p. 114599, Jun. 2024, doi: 10.1016/j.comptc.2024.114599.
[21] M. Akrom, S. Rustad, and H. K. Dipojono, "SMILES-based machine learning enables the prediction of corrosion inhibition capacity," *MRS Commun.*, vol. 14, no. 3, pp. 379–387, Apr. 2024, doi: 10.1557/s43579-024-00551-6.
[22] M. Akrom, S. Rustad, and H. K. Dipojono, "A machine learning approach to predict the efficiency of corrosion inhibition by natural product-based organic inhibitors," *Phys. Scr.*, vol. 99, no. 3, p. 036006, Mar. 2024, doi: 10.1088/1402-4896/ad28a9.
[23] J. A. Ingio, A. S. Nsang, and A. Iorliam, "Optimizing Rice Production Forecasting Through Integrating Multiple Linear Regression with Recursive Feature Elimination," *J. Futur. Artif. Intell. Technol.*, vol. 1, no. 2, pp. 96–108, Aug. 2024, doi: 10.62411/faith.2024-17.
[24] D. R. I. M. Setiadi, H. M. M. Islam, G. A. Trisnapradika, and W. Herowati, "Analyzing Preprocessing Impact on Machine Learning Classifiers for Cryotherapy and Immunotherapy Dataset," *J. Futur. Artif. Intell. Technol.*, vol. 1, no. 1, pp. 39–50, Jun. 2024, doi: 10.62411/faith.2024-2.
[25] I. Daniel, L. Akinyemi, and O. Udekwu, "Identifying Landslide Hotspots Using Unsupervised Clustering: A Case Study," *J. Futur. Artif. Intell. Technol.*, vol. 1, no. 3, pp. 249–268, Nov. 2024, doi: 10.62411/faith.3048-3719-37.
[26] P. Rebentrost, M. Mohseni, and S. Lloyd, "Quantum Support Vector Machine for Big Data Classification," *Phys. Rev. Lett.*, vol. 113, no. 13, p. 130503, Sep. 2014, doi: 10.1103/PhysRevLett.113.130503.
[27] M. Schuld, I. Sinayskiy, and F. Petruccione, "An introduction to quantum machine learning," *Contemp. Phys.*, vol. 56, no. 2, pp. 172–185, Apr. 2015, doi: 10.1080/00107514.2014.964942.
[28] V. Havlíček *et al.*, "Supervised learning with quantum-enhanced feature spaces," *Nature*, vol. 567, no. 7747, pp. 209–212, Mar. 2019, doi: 10.1038/s41586-019-0980-2.
[29] M. Schuld and N. Killoran, "Quantum Machine Learning in Feature Hilbert Spaces," *Phys. Rev. Lett.*, vol. 122, no. 4, p. 040504, Feb. 2019, doi: 10.1103/PhysRevLett.122.040504.
[30] M. Akrom *et al.*, "Quantum machine learning for corrosion resistance in stainless steel," *Mater. Today Quantum*, vol. 3, no. August, p. 100013, Sep. 2024, doi: 10.1016/j.mtquan.2024.100013.
[31] T. Sutojo, D. R. Ignatius, M. Setiadi, S. Rustad, W. Herowati, and M. Akrom, "Hybrid Quantum-Deep Learning Approach: Optimizing Land Cover Classification with GMM Outlier and Fusion Key Feature Selection," *Int. J. Intell. Eng. Syst.*, vol. 18, no. 1, pp. 638–648, Feb. 2025, doi: 10.22266/ijies2025.0229.45.
[32] P. O. Adebayo, F. Basaky, and E. Osaghae, "Leveraging Variational Quantum-Classical Algorithms for Enhanced Lung Cancer Prediction," *J. Comput. Theor. Appl.*, vol. 2, no. 3, pp. 307–323, Dec. 2024, doi: 10.62411/jcta.10424.
[33] S. M. Y. I. Tomal, A. Al Shafin, A. Afaf, and D. Bhattacharjee, "Quantum Convolutional Neural Network: A Hybrid Quantum-Classical Approach for Iris Dataset Classification," *J. Futur. Artif. Intell. Technol.*, vol. 1, no. 3, pp. 284–295, Dec. 2024, doi: 10.62411/faith.3048-3719-48.

[34] A. N. Safriandono, D. R. I. M. Setiadi, A. Dahlan, F. Z. Rahmanti, I. S. Wibisono, and A. A. Ojugo, "Analyzing Quantum Feature Engineering and Balancing Strategies Effect on Liver Disease Classification," *J. Futur. Artif. Intell. Technol.*, vol. 1, no. 1, pp. 51–63, Jun. 2024, doi: 10.62411/faith.2024-12.

[35] H.-Y. Huang *et al.*, "Power of data in quantum machine learning," *Nat. Commun.*, vol. 12, no. 1, p. 2631, May 2021, doi: 10.1038/s41467-021-22539-9.

[36] K. Mitarai, M. Negoro, M. Kitagawa, and K. Fujii, "Quantum circuit learning," *Phys. Rev. A*, vol. 98, no. 3, p. 032309, Sep. 2018, doi: 10.1103/PhysRevA.98.032309.

[37] M. Ahsan, M. Mahmud, P. Saha, K. Gupta, and Z. Siddique, "Effect of Data Scaling Methods on Machine Learning Algorithms and Model Performance," *Technologies*, vol. 9, no. 3, p. 52, Jul. 2021, doi: 10.3390/technologies9030052.

[38] M. Akrom, S. Rustad, A. G. Saputro, and H. K. Dipojono, "Data-driven investigation to model the corrosion inhibition efficiency of Pyrimidine-Pyrazole hybrid corrosion inhibitors," *Comput. Theor. Chem.*, vol. 1229, p. 114307, Nov. 2023, doi: 10.1016/j.comptc.2023.114307.

[39] M. Akrom, S. Rustad, and H. Kresno Dipojono, "Machine learning investigation to predict corrosion inhibition capacity of new amino acid compounds as corrosion inhibitors," *Results Chem.*, vol. 6, p. 101126, Dec. 2023, doi: 10.1016/j.rechem.2023.101126.

[40] C. C. Odiakaose *et al.*, "Hypertension Detection via Tree-Based Stack Ensemble with SMOTE-Tomek Data Balance and XGBoost Meta-Learner," *J. Futur. Artif. Intell. Technol.*, vol. 1, no. 3, pp. 269–283, Dec. 2024, doi: 10.62411/faith.3048-3719-43.

[41] M. Akrom, T. Sutojo, A. Pertiwi, S. Rustad, and H. Kresno Dipojono, "Investigation of Best QSPR-Based Machine Learning Model to Predict Corrosion Inhibition Performance of Pyridine-Quinoline Compounds," *J. Phys. Conf. Ser.*, vol. 2673, no. 1, p. 012014, Dec. 2023, doi: 10.1088/1742-6596/2673/1/012014.

[42] A. Botchkarev, "A New Typology Design of Performance Metrics to Measure Errors in Machine Learning Regression Algorithms," *Interdiscip. J. Information, Knowledge, Manag.*, vol. 14, pp. 045–076, 2019, doi: 10.28945/4184.

[43] M. Akrom, S. Rustad, A. G. Saputro, A. Ramelan, F. Fathurrahman, and H. K. Dipojono, "A combination of machine learning model and density functional theory method to predict corrosion inhibition performance of new diazine derivative compounds," *Mater. Today Commun.*, vol. 35, p. 106402, Jun. 2023, doi: 10.1016/j.mtcomm.2023.106402.

[44] E. I. Elsedimy, S. M. M. AboHashish, and F. Algarni, "New cardiovascular disease prediction approach using support vector machine and quantum-behaved particle swarm optimization," *Multimed. Tools Appl.*, vol. 83, no. 8, pp. 23901–23928, Aug. 2023, doi: 10.1007/s11042-023-16194-z.

[45] G. Abdulsalam, S. Meshoul, and H. Shaiba, "Explainable Heart Disease Prediction Using Ensemble-Quantum Machine Learning Approach," *Intell. Autom. Soft Comput.*, vol. 36, no. 1, pp. 761–779, 2023, doi: 10.32604/iasc.2023.032262.

[46] S. Jerbi, L. J. Fiderer, H. Poulsen Nautrup, J. M. Kübler, H. J. Briegel, and V. Dunjko, "Quantum machine learning beyond kernel methods," *Nat. Commun.*, vol. 14, no. 1, p. 517, Jan. 2023, doi: 10.1038/s41467-023-36159-y.

[47] X. Vasques, H. Paik, and L. Cif, "Application of quantum machine learning using quantum kernel algorithms on multiclass neuron M-type classification," *Sci. Rep.*, vol. 13, no. 1, p. 11541, Jul. 2023, doi: 10.1038/s41598-023-38558-z.

[48] D. Grimmer, I. Melgarejo-Lermas, J. Polo-Gómez, and E. Martín-Martínez, "Decoding quantum field theory with machine learning," *J. High Energy Phys.*, vol. 2023, no. 8, p. 31, Aug. 2023, doi: 10.1007/JHEP08(2023)031.

[49] J. D. Martín-Guerrero and L. Lamata, "Quantum Machine Learning: A tutorial," *Neurocomputing*, vol. 470, pp. 457–461, Jan. 2022, doi: 10.1016/j.neucom.2021.02.102.

[50] R. Narain, S. Saxena, and A. Goyal, "Cardiovascular risk prediction: a comparative study of Framingham and quantum neural network based approach," *Patient Prefer. Adherence*, vol. Volume 10, pp. 1259–1270, Jul. 2016, doi: 10.2147/PPA.S108203.

[51] O. Jaiyeoba, O. Jaiyeoba, E. Ogbuju, and F. Oladipo, "AI-Based Detection Techniques for Skin Diseases: A Review of Recent Methods, Datasets, Metrics, and Challenges," *J. Futur. Artif. Intell. Technol.*, vol. 1, no. 3, pp. 318–336, Dec. 2024, doi: 10.62411/faith.3048-3719-46.